BIOCHIMIE, 1974, 56, 967-985.

Model studies in relation to the molecular structure of chromatin (*).

Michel GOURÉVITCH, Pedro PUIGDOMÉNECH (**), Adrien CAVÉ, Gérard ETIENNE, Jean MÉRY and Joseph PARELLO.

Equipe de Recherche n° 140 (C.N.R.S.), Université des Sciences et Techniques du Languedoc, 34060 Montpellier, France.

Summary. — The paper reports a thermal denaturation analysis of calf thymus DNA associated with synthetic basic peptides (di-, tri-, and tetra-) including the X-X structure (basic doublet, X = Arg of Lys) which appears to be characteristic of the primary structure of all the known histones.

Analogies in thermal behaviour between peptides with a basic doublet structure and aliphatic diamines of the series $H_2N—(CH_2)_n—NH_2$, suggest that a positive doubly charged structure of defined length is crucial for the interaction with double stranded DNA.

A model is proposed for the interaction between histones and DNA on the basis of the above-mentioned intercharge distance requirement (diamine model), which is detailed in the case of the arginine-rich histone F2a1.

The role of the enzymatic acetylation and deacetylation of specific lysine residues in the case of arginine-rich histones is discussed in terms of the described diamine model. A possible role of the residue His 18 of histone F2a1 is considered in connection with this model.

Proton magnetic resonance studies of DNA associated with two model compounds, malouetine (a steroidal bis quaternary ammonium salt) and histidinamide, demonstrate that accurate description (magnetic, thermodynamic and kinetic) of the complexes can be obtained.

Preliminary results, using the analytical ultracentrifugation technique, in the case of some diamine complexes with circulary closed PM2 DNA are also reported.

INTRODUCTION.

Knowledge of histone-DNA interactions is important because of its relation to chromosome structure and gene regulation in higher organisms. Although their function is not precisely understood, histones are thought to be involved in the control of genetic activity. It has been pointed out that the role of histones is not merely to cover specific portions of DNA to be repressed with respect to protein synthesis, but also to help DNA to adopt precise conformations, such as those found in chromatin and chromosomes [1]. In fact, both aspects, funtional and structural, are certainly deeply interconnected.

The complex chemical composition of chromatin has so far prevented a detailed understanding of its organisation and function. A description of its gross organisation has been obtained through electron microscopy [2, 3] and X-ray diffraction studies [4, 5].

It appears that DNA adopts a tertiary structure by folding long stretches of double stranded DNA into more or less regular structure (for a discussion see J. A. Subirana in the present Symposium, and refs 6 and 7). The distribution of histones on the DNA in chromatin still remains obscure. The maintainance of the folded structure of DNA appears to be related to the presence of definite classes of histones in the complex (essentially the arginine rich histones F2a1 and F3) [4].

The heterogeneity in amino acid distribution along the sequences of histones certainly corresponds to a multiple functionality of the various proteins in the chromatin : DNA binding, protein-protein interaction, enzyme recognition, so that definite regions of these proteins could play distinct roles in the chromatin [8]. The study of model interactions between DNA and chromoso-

(*) Contribution n° 2 from the Equipe de Recherche n° 140 (C.N.R.S.). This work was presented by one of us (J.P.) at the Symposium on Chromosome Structure, organized by the Société de Chimie Biologique and the Délégation à la Recherche Scientifique et Technique, Strasbourg, 6-7th april 1974. This investigation was supported in part by the Délégation Générale à la Recherche Scientifique et Technique (Convention n° 73.7.1184).

(**) Permanent address : Instituto de Biologia Fundamental, Universidad Autonoma de Barcelona, Spain. Financial support from the C.S.I.C. (Spain) is greatly acknowledged.

mal proteins, protein fragments as well as synthetic peptides appears therefore to be a possible approach to the description of chromatin organization [9-12].

In the present study, representative peptides of the primary structure of histones have been selected. These include basic peptides (di-, tri and tetra-) with the X-X structure (basic doublet, X = Arg or Lys) and amino acid derivatives. Their association with DNA has been studied by thermal denaturation and proton NMR. The interaction between DNA and histones in the chromatin appears to include not only electrostatic forces between the negatively charged DNA phosphates and the basic groups of the proteins but also the participation of lower energy intermolecular forces such as hydrogen bonding and hydrophobic interactions [13]. The latter could be involved in processes of specific location of a given protein inside the DNA-protein complex, through interaction between nucleotides and amino acid residues.

NMR has proved to be very valuable for the description of molecular complexes in terms of intermolecular forces (electrostatic cohesion, hydrogen bonding, hydrophobic contact). Interactions studies of DNA and proteins, protein fragments and peptides have been reported using this technique [14-19]. The NMR analysis of the DNA-malouetine system (chosen because of its analogy with the peptide basic doublets) reported in this study has led to the full characterization of the complex.

The appearance of a DNA tertiary structure in chromatin is certainly related to local changes of the DNA secondary structure induced by histone-DNA interactions. A precise example of conformational dependence between DNA tertiary structure and a localized alteration in the secondary structure is afforded by the interaction between intercalating ligands and supercoiled circularly closed DNA's [20, 21]. It has been suggested that supercoiled, but not necessarily circular DNA, is involved in structural and functional units in the chromosomes of higher organisms [1]. The study of model interaction between circularly closed DNA's and purified chromosomal components or analogs appears therefore to be relevant to the study of chromatin organization. Details of the interaction between SV40 DNA and histone F2al have already been published [22]. An analysis of the binding of two aliphatic diamines (H_2N—$(CH_2)_n$—NH_2, n = 10 and 12) and decamethonium to bacteriophage PM2 DNA is reported using analytical ultracentrifugation. These dicationic ligands were selected because of structural analogies with defined sequence regions of histones.

MATERIALS AND METHODS.

1 — *Preparation of DNA samples.*

Calf thymus DNA was prepared following the classical method of Marmur [23]. Ultrasonic degradation of a DNA solution (1 mg/ml) in 0.017 M sodium citrate pH 6.5 containing 0.15 M NaCl was carried out, using a 100 watt MSE ultrasonic desintegrator for 10 mn at 4°C. DNA was precipitated by adding two volumes of cold ethanol 95° and centrifuged. After drying exhaustively under vacuum, sonicated DNA was recovered with a 92 p. cent yield.

Bacteriophage PM2 DNA was kindly provided by Dr. B. Révêt (Institut de Recherches Scientifiques sur le Cancer, Villejuif, France). All preprations used here contained more than 80 p. cent closed circular molecules. DNA samples were characterized by standard hydrodynamic as well as optical properties (see Results). DNA concentrations were determined by absorbance measurements at 260 mn. A value of $A_{260} = 20.0$ for 1 mg DNA/ml was adopted.

2 — Ligands.

Aliphatic amines. Commercial reagents (Fluka, Buchs, Switzerland) were used without further purification. All amines not already supplied as salts (diamines H_2N—$(CH_2)_n$ — NH_2 with n = 3, 7, 8, 9, 10, 12 as well as 1-aminopentane) were dissolved in spectral grad methanol and neutralized exactly using a methanolic HCl solution. Exhaustive drying under vacuum afforded the corresponding hydrochlorides.

Quaternary ammonium salts. Decamethonium bromide was a commercial reagent (Fluka). Malouetine chloride, a bis-quaternary steroidal ammonium salt, was kindly provided by Dr. F. Khuong-Huu Lainé. (Institut de Chimie des Substances Naturelles, Gif, France). *Peptides and derivatives.* Lys-Lys triacetate and Arg-Lys diacetate commercial products from Cyclo Chemical (U.S.A.) were purified by chromatography using a Dovex 50-X4 ionic exchange resin. Ac-Gly-Arg-Arg-GlyOCH_3 dihydrochloride (peptide I) and Ac-Gly-Arg-GlyOCH_3 hydrochloride (peptide II) were synthesized by means of the Merrifield solid phase technique [24] using classical reagents and protective groups (*). The final purity of both syn-

(*) Full details will be published elsewhere.

thetic peptides was checked by paper electrophoresis, chromatography, amino-acid analysis and field desorption mass spectrometry [25]. Histidinamide hydrochloride was a gift from the Centre de Biochimie Macromoléculaire (C.N.R.S., Montpellier, France).

Ligands were dissolved in appropriate buffer solutions and their concentration was determined either by weighing or by amino acid analysis in the case of peptides.

3 — PROCEDURES.

Thermal denaturation studies of ligand-DNA complexes were carried out using a 2 mM phosphate buffer pH 6.9 (room temperature) 0.02 mM in Na_2-EDTA, and 0.075 mM DNA-P. Complexes were prepared by mixing 0.15 mM DNA-phosphate (DNA-P) and variable concentrations of a given ligand in equal volumes. Controls at 400 nm were performed in order to detect any contribution of the turbidity effect to the measured absorbance. Measurements were carried out at 258 nm using a Gilford 2400 spectrophotometer equipped with a variable temperature device. A linear temperature increase of 0.4°/mn was maintained between 25°C and 100°C. Solutions were previously saturated with wet helium gas before transfer to cuvettes. Four cells were used in the spectrophotometer block, one containing phosphate buffer only, an other a DNA solution in order to define T_m° (melting temperature of free DNA). The two remaining were filled with ligand-DNA complexes of different R_c ratios (number of ligand positive charges per number of DNA-phosphate negative charges ; R denotes the molar ratio). No correction for volume expansion was included at this stage. All thermal transition curves are described by means of three parameters : (i)ΔH_{258}, maximal hyperchromicity at 258 nm representing the fraction of the total absorbance change from the reading at room temperature (*ca* 22°C) to the high-temperature plateau value (at any temperature, hyperchromicity is defined as $H_{258}(t) = 100 \times [A_{258}(t°) - A_{258}(22°)/A_{258}(22°)]$ (ii) T_m, melting temperature in degrees corresponding to the transition mid-point temperature, so that $H_{258}(T_m) = \Delta H_{258}/2$ and (iii) $\sigma_{1/2}$, transition half-width in degrees measured between 0.25 and 0.75 of maximal hyperchromicity. For each R_c value, the variation of melting temperature between the ligand-DNA complex and the free DNA is defined by $\Delta T_m = T_m - T_m^\circ$

Analytical ultracentrifugation (at 35,000 rpm) was carried out using a MSE ultracentrifuge (1968 model) equipped with a four cell rotor, ultraviolet absorption optics and a scanner device for direct recording of absorbance. Complexes were prepared following the method of Waring [26] in which successive increments of a ligand solution (*ca* 10 µl) were added to the cell containing 0.35 ml of PM2 DNA with an absorbance of 0.75 at 260 nm. The same DNA sample was used for up to 15 sedimentation runs at increasing ligand concentrations (the samples were shaken for 20 mn after the addition of the ligand). Sedimentation coefficients were measured according to standard procedures. S_{20} values were directly determined and they have not been corrected for viscosity, buoyancy or DNA concentration.

Proton NMR spectra, were recorded around 30°C using 5 mm precision tubes, under continuous wave (CW) conditions in a Varian HA-100 spectrometer equipped with a C.A.T. Varian C-1024 device to improve the signal to noise ratio (Laboratoire de Mesures Physiques, U.S.T.L. Montpellier). Variable temperature experiments were carried out using a V-6040 temperature control device. In order to define the relative amounts of ligand and DNA molecules as precisely as possible, the following procedure was adopted. The total amount of ligand was carefully weighed and dissolved in a given volume of H_2O. Variable portions of this solution were then lyophylized in order to get increasing amounts of well dried ligand. A sonicated calf thymus DNA solution was prepared using a D_2O-phosphate buffer. Aliquots (0.5 ml) were then poured onto the lyophylized residues, so that D_2O solutions were obtained with a constant DNA concentration and variable ligand concentrations. The solvant signal (residual HDO) was used as an homonuclear proton internal lock signal. When indicated chemical shifts quoted in Hz referred to internal DSS (sodium 2,2-dimethyl-2-silapentane-5-sulfonate). Signal half widths are measured in Hz. D corresponds to the observed half-width for a given value of the ligand to DNA ratio R. When $R = 0$ or ∞ the half-width is designated by d and Δ respectively. In the case of malouetine-DNA complexes, signals corresponding to the N-trimethyl groups (at positions 3 and 20 respectively, see formula in fig. 9) are mutually overlapping, as well as those corresponding to the C-methyl groups (at positions 18 and 19, see formula in fig. 9). In order to evaluate the relative contribution of each component to the whole signal, the experimental curves (see for instance fig. 10) were adjusted by means of a least square fitting treatment. Calculations including a set of R values afforded a nearly linear relationship between D_g (global half-width of the com-

posite signal) and D (average half-width of both components) which was used in order to get D values from experimental ones Dg. In the case of histidinamide-DNA complexes spin decoupling conditions (double and triple resonance) were used in order to eliminate spin-spin coupling contribution to the signal half-width.

RESULTS.

I. — *Thermal denaturation studies.*

The interaction of DNA basic ligands was investigated, by means of helix to coil transition absorbance-temperature profiles. We examined the thermal denaturation of sonicated calf thymus associated with hydrochlorides of basic peptides Arg-Lys, Lys-Lys, Ac-Gly-Arg-Arg-GlyOCH$_3$ (peptide I), Ac-Gly-Arg-GlyOCH$_3$ (peptide II) of a series of aliphatic diamines, H_2N-$(CH_2)_n$-NH_2 (n = 2-10, 12) as well as decamethonium bromide, malouetine chloride and 1-aminopentane hydrochloride. In all the cases, the observed thermal

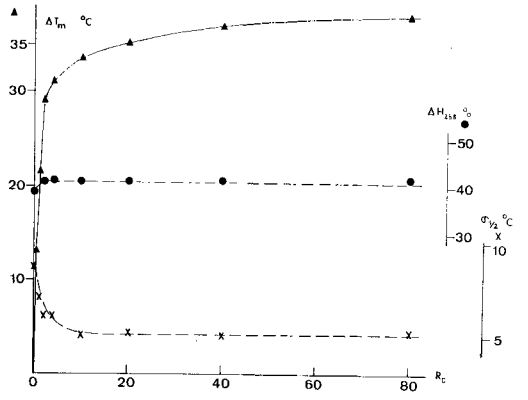

FIG. 1. — *Thermal denaturation parameters versus R_c* (ratio of the number of ligand positive charges to the number of negative DNA-phosphate charges) for the DNA/1,5-diaminopentane dihydrochloride complex (sonicated calf thymus DNA) in phosphate buffer, KH_2PO_4 0.5 mM, Na_2HPO_4 0.5 mM, Na_2-EDTA 0.02 mM, pH 6.9 (room temperature) ; [DNA-P] = 0.075 mM. Symbols : (▲) melting temperature variation ΔT_m ; (●) hyperchromicity ΔH_{258} ; (×) transition half-width $\sigma_{1/2}$.

profiles were unimodal. However, when using a derivative representation $dH_{258}/dt = f(t)$, it clearly appears that the thermal profiles are composite with different definite transitions owing to DNA sequence heterogeneity. Nevertheless, thermal transitions were characterized by the global parameters T_m, ΔH_{258} and $\sigma_{1/2}$ (for definitions see Materials and Methods). Under the present conditions of ionic strength (2.0 mM) and pH (6.9) free sonicated DNA shows a thermal transition with $T^\circ_M = 51 \pm 0.5$°C, $\Delta H^\circ_{258} = 39 \pm 1$ p. cent and $\sigma^\circ_{1/2} = 8.5 \pm 0.5$°C, whereas with free native DNA $T^\circ_m = 54$-55°C, $\Delta H^\circ_{258} = 36$-37 p. cent and $\sigma^\circ_{1/2} \parallel 6.0$°C (*). The lowering of T_m between native DNA (M_w *ca* 7.8 × 10^6 daltons) and sonicated DNA

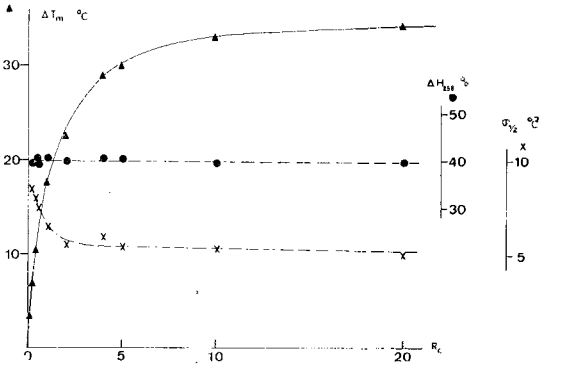

FIG. 2. — *Thermal denaturation parameters versus R_c for the DNA/Lys-Lys complex.* Conditions and symbols are identical to those in fig. 1.

(M_w *ca* 2.6 × 10^5 daltons) is in agreement with experimental as well as theoretical results [27, 28] (**). Two main types of thermal behaviour may be distinguished :

1) ΔT_m reaches a constant value ΔT_M as R increases. Figures 1 and 2 are representative of this typical saturation profile, which is observed for all the aliphatic diamines of the series n = 2-10 as well for the dibasic peptides considered. In general, ΔH_{258} remains constant throughout the saturation process, whereas $\sigma_{1/2}$ decreases from $\sigma^\circ_{1/2}$ to a lower saturation value.

2) ΔT_m reaches a maximum and decreases on either side of this optimum. This is the case of 1,12-diaminododecane (fig. 3), malouetine (fig. 4) and peptide II. The parameters ΔH_{258} and $\sigma_{1/2}$ can be either independent of R_c (peptide II), or greatly dependent on it. For instance, in the case of 1,12-diaminododecane, ΔH_{258} first decreases (*ca* 30 p. cent) and then increases to very high values (*ca* 55 p. cent) when R_c is varied from 0 to 40 (fig.

(*) The superscript symbol ° is used in order to characterize the DNA free state ($R_c = 0$).

(**) T_m versus ionic strength (log of Na^+ concentration) shows that native and sonicated DNA yield linear plots. The slope of the latter appears greater than that of the former, so that the T_m difference between both DNA states is disminished as the ionic strength is increased (unpublished result from our laboratory).

3). This abnormal behaviour is certainly related to aggregation processes, a situation which manifests itself by contribution of scattering to the absorption of light. Nevertheless, the transition

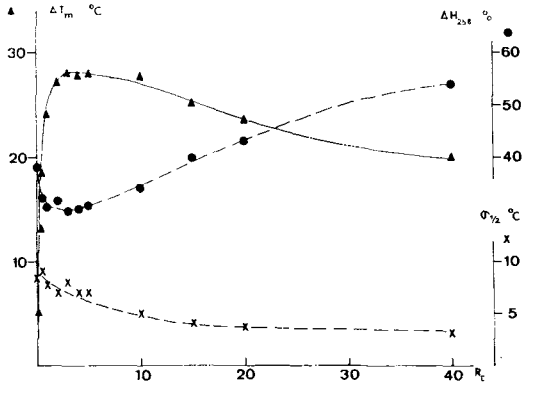

FIG. 3. — *Thermal denaturation parameters versus R_c for the DNA/1,12-diaminododecane dihydrochloride complex.* Conditions and symbols are identical to those in fig. 1.

half-width $\sigma_{1/2}$ shows a similar variation (fig. 3) to that of ligands with a typical saturation behaviour (fig. 1 and 2).

In the case of malouetine, ΔH_{258} rapidly decreases when R_c increases, so that no thermal transition is detectable for R_c greater than 20. This observation is in agreement with previous results dealing with thermal helix to coil transition profiles of malouetine-DNA complexes [29]. The appearance of a ΔT_m maximum value when R_c *ca* 2 (fig. 4) was not noticed previously, as the corresponding studies were restricted to lower values of R_c [29]. The profiles ΔT_m versus R_c were analyzed by means of the empirical equation (I), $\Delta T_m = (\Delta T_M \times R_c)/(K + R_c)$ as previously proposed by Mahler and Mehrotra [30] in their thermal denaturation studies on aliphatic diamine-DNA complexes (K is a dimensionless constant, so that when $R_c = K$, $\Delta T_m = \Delta T_M/2$).

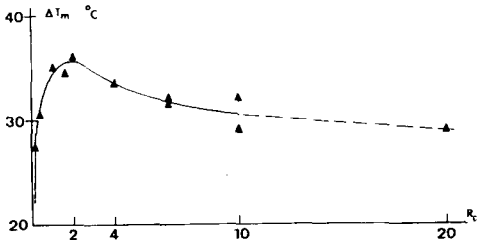

FIG. 4. — *Melting temperature variation ΔT_m versus R_c for the DNA-malouetine chloride complex.* Conditions and symbols are identical to those in fig. 1.

A similar quantitative treatment was proposed by Brown when analyzing the thermal profiles of complexes between DNA and basic dipeptide methyl esters [11]. Equation (I) is readily converted into the linear double reciprocal form (II), $\Delta T_m^{-1} = \Delta T_M^{-1} + K (\Delta T_M^{-1} \times R_c^{-1})$. Experimental data were analyzed by means of a least square programme. Except for single charge structures (peptide I and 1-aminopentane), a good correlation was found in most cases. Correlation coefficients better than 0.99 were observed in all but a few cases (values between brackets in table I). Strictly speaking, a quantitative approach is not possible

TABLE I.

Ligand		ΔT_M °C	K
$H_2N-(CH_2)_n-NH_2$	n = 2	33.6	3.0
	n = 3	(36.3)	(0.9)
	n = 4	37.4	1.0
	n = 5	37.7	0.8
	n = 6	35.7	0.9
	n = 7	34.7	0.8
	n = 8	32.7	0.9
	n = 9	(29.5)	(0.6)
	n = 10	27.6	0.8
	n = 12	42.5	0.7
Malouetine		37.9	0.09
Decamethonium		(25.6)	(1.0)
Lys—Lys		34.6	1.7
Arg—Lys		30.4	1.2
Ac—Gly—Arg—Arg—$GlyOCH_3$		23.9	0.22

for curves such as those obtained for 1, 12-diaminododecane (fig. 3) and malouetine (fig. 4) which deviate from a typical saturation profile. If it is assumed that two types of complexes are indeed present, the part of the curve corresponding to lower R_c values can be analyzed by means of the above mentioned equation. In both cases, R_c values were selected in the range between 0.05 and 1.0.

II — *Analytical ultracentrifugation studies.*

The effects of four dicationic ligands on the sedimentation coefficient of circular PM2 DNA are presented in figures 5 to 8. The removal and reversal of supercoils of PM2 DNA when interacting with malouetine has been recently described by Waring and Chisholm [31]. The present results (see fig. 8) were obtained using higher ionic strength conditions and were established for the sake of comparison with NMR results (see below). Decamethonium has no uncoiling effect on circular DNA, at least for R $\leqslant$ 100 (ligand to nucleotide ratio), whereas malouetine gives an uncoiling effect at R *ca* 0.8 under similar ionic conditions [31]. Both compounds nevertheless appear closely related structurally, as far as the dicationic arran-

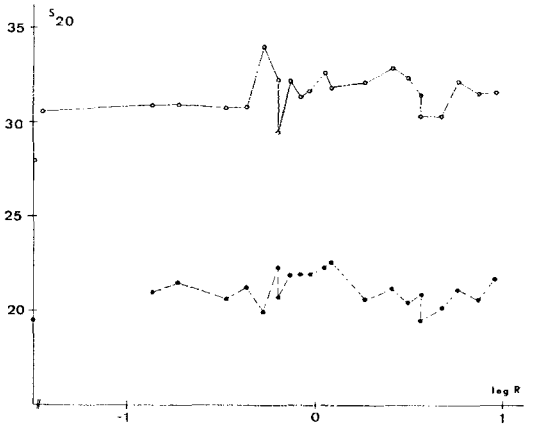

FIG. 5. — *Effect of 1,10-diaminodecane dihydrochloride on the sedimentation coefficient of PM2 DNA in tris buffer 24 mM, Na_2-EDTA 0.05 mM, pH 7.5.* R represents the input ratio of added ligand to DNA nucleotides. Open symbols are reserved for closed circular duplex molecules, whereas closed symbols are characteristic of the nicked circular molecules present in the DNA preparation. Sedimentation coefficient S_{20} are uncorrected values determined directly at 20°C.

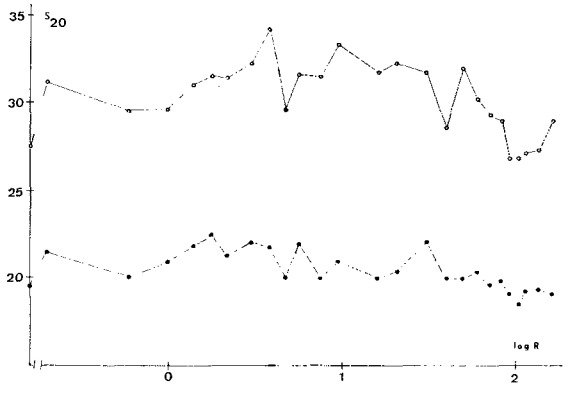

FIG. 6. — *Effect of decamethonium bromide on the sedimentation coefficient of PM2 DNA.* Conditions and symbols employed are the same as in figure 5.

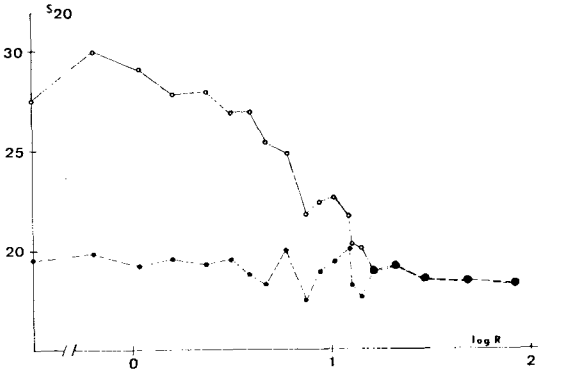

FIG. 7. — *Effect of 1,12-diaminododecane dihydrochloride on the sedimentation coefficient of PM2 DNA, in phosphate buffer,* KH_2PO_4 5 mM, K_2HPO_4 5 mM, Na_2-EDTA 1 mM, pH 6.85. The same symbols as in fig. 5 are used. Larger closed symbols correspond to weight average S_{20} values from a single boundary formed by closed and nicked circles sedimenting together.

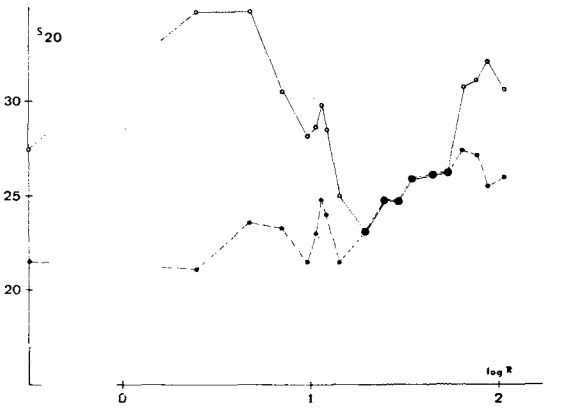

FIG. 8. — *Effect of malouetine (chloride) on the sedimentation coefficient of PM2 DNA, in phosphate buffer,* KH_2PO_4 25 mM, K_2HPO_4 25 mM, Na_2-EDTA 1 mM, NaCl 0.1 M, pH 6.5. The same symbols as in figures 5 and 7 are used.

gement is concerned. 1,10-diaminodecane has a behaviour similar to that observed for decamethonium (see fig. 5). However, when 1,12-diaminododecane is allowed to interact with PM2 DNA, removal of supercoiling is observed. In comparison to malouetine, the equivalence region for

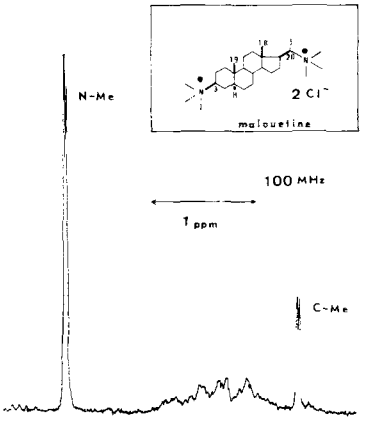

FIG. 9. — *100 MHz CW ^1H NMR spectrum at 27°C of 42 mM malouetine (chloride) in D_2O.*

which closed and nicked circular DNA molecules present identical S_{20} values, appears more spread out and no phase of supercoil regeneration was reached even for ratios up to 100. It was checked that no important transformation from the circularly closed form to the nicked one had occured during the experiments.

III — NMR STUDIES.

Malouetine-DNA system.

When malouetine was added to sonicated calf thymus DNA in D_2O phosphate buffer at constant concentration, half-width variations of the signals in the malouetine NMR spectrum were observed. Two main groups of signals were selected for quantitative treatment because of their relative simplicity (see figures 9 and 10) : the one at higher field corresponds to the proton resonances of the angular methyl groups 18 and 19, the other at lower field to those of both the N-trimethyl groups at positions 3 and 20. Signal overlapping was observed in both cases, the chemical shift differences being less than the signal half-widths. However, as described in Materials and Methods a convenient procedure can be applied to evaluate the contribution of each component to the whole signal. For the C-Me resonances and the N-Me resonances, only an average half-width value D could be defined, and this was linearly related to the global half-widtf D_g of the composite signal. An NMR binding isotherm was obtained by plotting R, ligand to nucleotide molar ratio, versus $(D-d)^{-1}$ where d represents the half-width when R = O. Two very distinct curves are observed in figure 11 for the C-Me and N-Me groups respectively, a fact

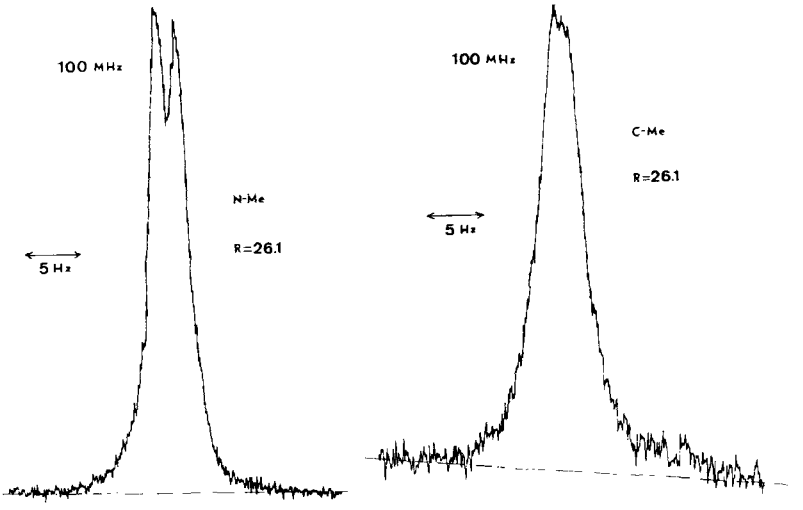

FIG. 10. — *100 MHz CW ^1H NMR spectrum at 40°C of malouetine-DNA complex (sonicated calf thymus DNA)*, for R = 26.1 (input ratio of added ligand to DNA nucleotides). [DNA-P] = 1.01 mM, in D_2O-phosphate buffer, KH_2PO_4 8.6 mM, K_2HPO_4 29.6 mM, Na_2-EDTA 0.93 mM, NaCl 0.101 M, pD *ca* 7.5. Right : expanded region related to the C-Me group resonances. Left : expanded region related to the N-Me group resonances.

which clearly indicates that nuclear relaxation appears to be quite different for each ligand proton type when associated to DNA. The larger relaxation rate is observed for the C-Me group which are located in a very hydrophobic part of

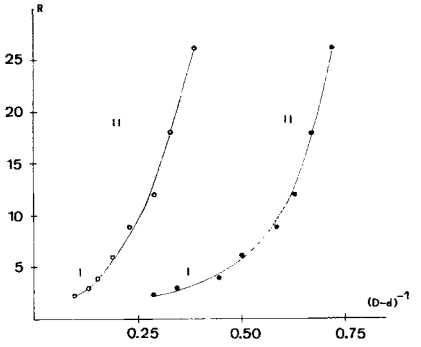

FIG. 11. — *NMR binding isotherm R versus (D-d)⁻¹ at 40°C for the malouetine-DNA system.* Open symbols and closed ones respectively represent the C-Me and the N-Me ligand groups. Sonicated calf thymus DNA concentration is held constant at 1.01 mM. Ionic conditions are the same as in fig. 10. NMR frequency : 100 MHz.

the molecule, in comparison with N-Me groups which belong to the polar part of it. Relaxation difference was still more pronounced when the malouetine-DNA system was analyzed under variable temperature conditions as shown in figure 12. A very salient feature in figure 11 is the fact that R versus $(D-d)^{-1}$ plots are non-linear. Interactions between drugs and proteins usually give linear plots, a situation which corresponds to the existence of a defined class of binding sites, and is characterized through a linear Scatchard representation.

Departure from linearity in figure 11 (upward curvature) could be due, either to the presence of a single type of complex satisfying the conditions of neighbouring exclusion as defined by Crothers [32] or to the presence of more than one type of complex. A quantitative analysis of the malouetine-DNA system makes it likely that two types of complexes do exist. A fact which is in agreement with the thermal denaturation results reported in figure 4. A thermal stabilizing complex I is defined at lower ratios (R less than 5) whereas a less thermal stabilizing complex II appears at higher ratios. It is particularly interesting to note that in complex I the C-Me and N-Me relaxation rates differ markedly ($\Delta_{C\text{-}Me}/\Delta_{N\text{-}Me}$ *ca* 3.7) (see table II). A possible explanation is to assume that the most bulky face of the steroid ligand is in close contact with

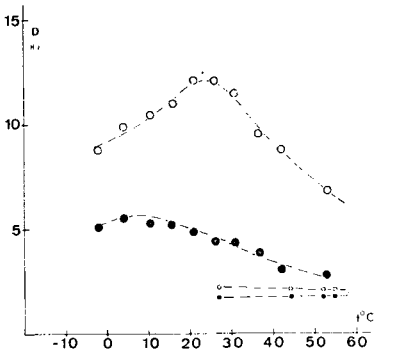

FIG. 12. — *Effect of temperature on the 100 MHz NMR signal half-width D for the malouetine-DNA system when R = 3.70 and [DNA-P] = 3.54 mM.* Ionic conditions are as in legend for fig. 10. Open and closed symbols are related to C-Me and N-Me resonances respectively. Lower curves between 25° and 55°C correspond to half-width d variation when [DNA-P] = O and [malouetine] = 10 mM under similar ionic conditions (open and closed symbols represent C-Me and N-Me resonances respectively).

TABLE II.

Characteristic magnetic and thermodynamic parameters for malouetine- and histidinamide-DNA complexes determined by NMR. (a) following method 1 and (b) method 2.

	Relaxation rate Δ in Hz		Thermodynamic parameters
Malouetine (complex I)	220	(C-Me)	K_d (40°) = 2×10^{-2} M (a) K_d (40°) = 9×10^{-2} M (b)
μ *ca* 2×10^{-1} M	60	(N-Me)	$\Delta H_{40°}$ *ca* 8 Kcal/mole
	$\Delta_{C\text{-}Me}/\Delta_{N\text{-}Me} = 3.7$		
Histidinamide	10	(C_4-H)	K_d (27°) = 6×10^{-2} M (a)
μ *ca* 2×10^{-3} M	16	(β-CH_2)	K_d (27°) = 3×10^{-2} M (b)
			$\Delta H_{27°}$ *ca* 7.5 Kcal/mole

the DNA molecule. Cohesion could be partly due to hydrophobic contact between elements of both molecules.

Furthermore, if D_g is measured under isotherm conditions at different NMR frequencies (100 MHz and 60 MHz) it can be concluded that complex formation between DNA and malouetine is not characterized by any significant chemical shift effect. This observation probably excludes a close proximity between DNA bases and the C-Me groups of malouetine, yielding complex cohesion through aliphatic-aromatic interactions as found in the tertiary structures of proteins (see [33] and references quoted herein). In particular, an intercalation type complex appears to be very unlikely on the basis of this experimental evidence. This interpretation is in full agreement with previous conclusions derived from interactions studies of steroidal diamines with nucleic acids [34, 35].

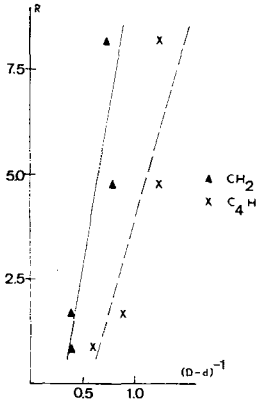

FIG. 13. — *NMR binding isotherm R versus $(D-d)^{-1}$ at 27°C in the case of the histidinamide-DNA system.* Sonicated calf thymus concentration is held constant at [DNA-P] = 12.6 mM, in D_2O-phosphate buffer KH_2PO_4 0.5 mM, Na_2HPO_4 0.5 mM, Na_2-EDTA 0.02 mM. D is measured under triple irradiation conditions (see Materials and Methods). NMR frequency: 100 MHz.

Histidinamide-DNA system.

Complexes of histidinamide with sonicated calf thymus DNA were also studied by proton NMR at 100 MHz. Experiments were carried out at low ionic strength (2.0 mM) because of the reduced affinity of the ligand for double stranded DNA. NMR binding isotherms (figures 13 and 14) as well as variable temperature experiments (fig. 15) clearly indicate that the imidazole protons (C_2-H and C_4-H) differ markedly from other protons in the side-chain (β-CH_2) in relaxation as well as chemical shift effects. Particularly outstanding is the observation of downfield chemical shift effects when histidinamide interacts with double stranded DNA. These results suggest that the imidazole moiety could interact with DNA bases through hydrogen bonding (see discussion). However, a

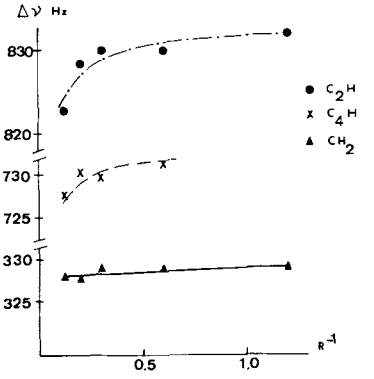

FIG. 14. — *Chemical shift variations (Hz) of three distinct proton groups of histidinamide at 27°C* β-CH_2, C_4-H and C_2-H, when interacting with calf thymus sonicated DNA. [DNA-P] = 12.6 mM. pD = 5.62 ± 0.07. Chemical shifts are referred to internal DSS. Temperature and ionic conditions are the same as in fig. 13.

downfield shift could also be interpreted as the consequence of an histidinamide pK variation under the influence of negatively charged DNA phosphate groups, even if the pH is held constant at 5.62 ± 0.07.

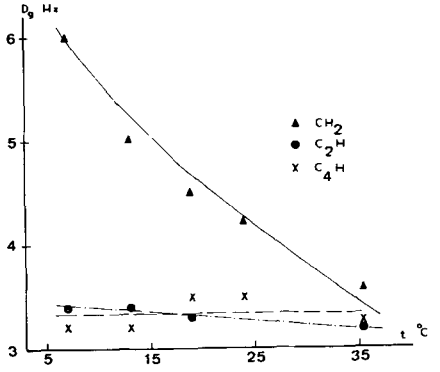

FIG. 15. — *Effect of temperature on the global half-width Dg (no irradiation conditions were used) for three distinct proton groups of histidinamide,* interacting with sonicated calf thymus DNA, when R = 1.65. Conditions are identical to those in figs 15 and 16.

Changes in signal half-width appear to be important for protons in the β-CH_2 group, whereas no changes of either imidazole protons were obser-

ved when the temperature was varied (fig. 15). The experiments, performed at a single frequency (100 MHz) do not allow one to distinguish between relaxation and chemical shift effects, because of the possibility of a non-equivalence between the protons in the β-CH_2 group when interaction of histidinamide with DNA takes place.

Quantitative treatment of NMR data.

a) *Determination of dissociation constants K_d (see table II).*

Method 1. — Binding isotherms, R versus $(D-d)^{-1}$ were analyzed by means of equation (III) which has been widely used in NMR studies of ligand-protein interactions [36],

$$(III) \qquad R = n\,\frac{\Delta - d}{D - d} - \frac{K_d}{A_0}$$

Method 2. Under rapid exchange conditions, temperature dependent half-width variations were analyzed according to the Van't Hoff principle, assuming that the relaxation parameters and the complex formation enthalpies remained constant in the temperature range considered (between 25° and 55°C). Dissociation constants were then calculated for a given temperature.

b) *Determination of magnetic parameters.*

According to equation (III) the slope of a linear isotherm R versus $(D-d)^{-1}$ yields the relaxation rate of a given group of ligand nucleic in the complex, provided the stoichiometry ratio is known. For a given molecule the ratio between values characteristic of two distinct groups of nuclei is independent of n. Ratios instead of absolute values were often used to characterize complex formation [37]. For the malouetine-DNA system, the value n = 0.25 was adopted according to previous results by Mahler *et al* [34] based on UV spectroscopy evidence. For the histinamide-DNA system the assumed value was 1.

TABLE III.

Basic clustering in histones of known sequence from calf thymus.

Histone	M (a)	N (b)	N/M	p (c)
F2a1.....	102	25 (27)	0.245 (0.205)	60.0 ($p_2 = 48.0$; $p_3 = 12.0$ (59.3) ($p_2 = 29.6$; $p_3 = 11.1$; $p_5 = 18.5$)
F3.....	135	31 (33)	0.230 (0.244)	51.6 ($p_2 = 51.6$) (54.5) ($p_2 = 54.5$)
F2a2.....	129	26 (30)	0.201 (0.232)	23.07 ($p_2 = 23.07$) 43.3 ($p_2 = 33.3$; $p_3 = 10.0$)
F2b.....	125	28 (31)	0.224 (0.248)	53.6 ($p_2 = 35.8$; $p_5 = 17.9$) (54.8) ($p_2 = 38.8$; $p_5 = 16.1$)
F1.....	108 (d)	22	0.204	50.0 ($p_2 = 18.2$; $p_3 = 13.6$; $p_4 = 18.2$

(a) M = total number of residues.

(b) N = total number of basic residues (Arg and Lys). Figures between brackets include His as a basic residue (F1 histone has no His residue).

(c) p = percentage of basic clustering defined by $\sum_{n=2}^{N} \frac{m \times n}{N} = \sum_{n=2}^{N} p_n$. m is the number of basic multiplets with multiplicity n.

(d) The 108 residues correspond to the NH_2- terminal half of rabbit thymus F1 histone component RTL-3 the sequence of which was determined by Jones and Cole [41].

Symbols are as follows : R ligand to nucleotide molar ratio, n number of binding sites per nucleotide, D signal half-width for a given R value (d and Δ are the corresponding half-widths when R = 0 and R = ∞), K_d complex dissociation constant, A_0 nucleotide molar concentration.

For the binding isotherms of figure 11 only the complex I region was tentatively analyzed by means of equation (III).

c) *Kinetic information.*

When the malouetine-DNA system was analyzed under variable temperature conditions, it was observed that half-widths reached a maximum value in the temperature range between 10 and

25°C (see fig. 12). The general shape of the experimental curves could be predicted satisfactorily by assuming a ligand exchange between two states free and DNA-bound. Both observed maxima (C-Me and N-Me signals) correspond to kinetic transition points. At lower temperatures the exchange is slow on the NMR time scale, whereas it is rapid at higher temperatures.

An accurate quantitative analysis of the curves in figure 12 could not be obtained on the basis of a classical NMR exchange formalism [38], because of the contribution of uncontrolled viscosity effects to the whole phenomenon.

However, an estimation of complex average lifetimes could be achieved : less than 1 msec at temperatures higher than 20°C. For the histidinamide-DNA system, the exchange process was always rapid in the temperature range considered (see fig. 15).

DISCUSSION.

I.— *The role of clustering of the basic residues in the primary structure of histones.*

It has been largely emphasized during the establishment of the primary structure of the main histone fractions from calf thymus chromatin that the basic residues Arg and Lys are concentrated in well defined zones of the sequence and that highly basic clustered regions are observed [39]. The situation is presented in a quantitative way in table III. Basic multiplets are defined as partial sequences of the type X_n, where X = Arg or Lys and $n \geq 2$. In general, the clustering percentage p presents a value higher than 50 p. cent. The observed distribution of basic multiplets deviates significantly from expected values on the basis of a random building process of the sequence, at least in the case of histones F2a1 and F2b [40]. As indicated in table III, the most frequently observed basic multiplets are the doublets (n = 2) Arg-Arg, Arg-Lys, Lys-Arg, and Lys-Lys. Peptides including a basic doublet therefore appear to be very suitable models to study interactions involving the histone basic regions in histone-DNA complexes.

Two basic peptides, Ac-Gly-Arg-Arg-GlyOCH$_3$ (peptide I) and Ac-Gly-Arg-GlyOCH$_3$ (peptide II) were selected. The corresponding DNA-complexe differ markedly in their thermal behaviour, as shown in figure 16. Peptide I-DNA complex rapidly reaches the saturation value, $\Delta T_M = 24°$ (see table I) when R_c is increased. More than 80 p. cent of the total saturation value is achieved when $R_c = 1$, whereas peptide II-DNA complex only reaches about 20 p. cent of the total stabilization. For the purposes of comparison, figure 16 also describes the thermal behaviour of DNA complexes with 1,5-diaminopentane and 1-aminopentane. The monobasic ligand affords a very low stabilizing capacity when compared to the dibasic one. According to chromatin composition (see table IV) it appears that R_c values are certainly lower than 1 in the nucleohistone complex. Under these conditions a protein basic doublet would be able to stabilize the secondary structure of double

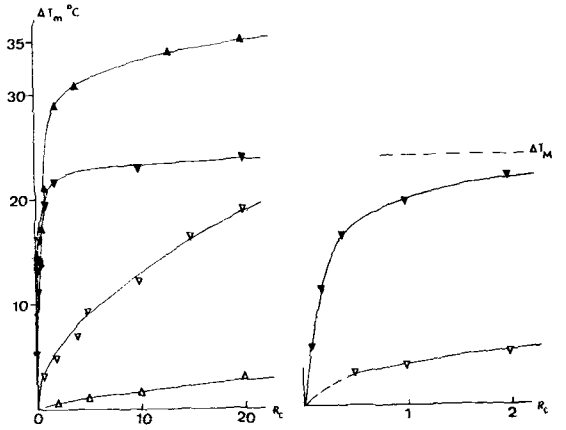

FIG. 16. — *Compared saturation profiles for sonicated calf thymus DNA associated* with (▲) 1,5-diaminopentane, (△) 1-aminopentane, (▼) Ac-Gly-Arg-Arg-Gly OCH_3 and (▽) Ac-Gly-Arg-Gly OCH_3. Left part : $0 \leq R_c \leq 20$. Right part : expanded scale $0 \leq R_c \leq 2$ for the two latter peptide ligands. Conditions are as described in the legend to fig. 1 as well as in Materials and Methods.

stranded DNA much more efficiently than a singlet structure. A similar result was obtained by Brown [11] when analyzing the thermal behaviour of DNA complexes with basic dipeptides methyl esters. Monobasic peptides with one Arg residue appeared less efficient at stabilizing the DNA structure than a dipeptide with two Arg residues. Very closely related results were recently obtained by Gabbay *et al* [18] using lysyl tripeptides. The dilysyl peptides increased the T_m to a greater extent than did the monolysyl ones. Furthermore, on the basis of equilibrium dialysis the same authors showed that the dilysyl systems had an enhanced affinity for helical DNA when the two lysyl residues were adjacent to one another. It can therefore be assumed that the basic multiplets observed in the primary structures of histones certainly act as preferred regions for direct elec-

trostatic interaction with the DNA phosphate backbone.

If calculations are performed taking into account chromatin composition (*) and features of histone primary structure (see table IV) it results in a maximum neutralization of *ca* 73 p. cent of the DNA-phosphate groups if all the histone positive charges were interacting. Only 35 p. cent of the phosphate groups are able to interact with protein basic multiplet structures as defined in table III. In fact, Arg and Lys often appear in highly basic regions although they do not correspond to the above mentioned definition. The situation is particularly noticeable in the case of histone F2a2, for which p = 23 p. cent (see table III). Nevertheless, as pointed out by Sautière *et al.* [43] very basic regions are observed in the primary structure of this protein, such as *Lys*-Ala-*Arg*-Ala-*Lys*-Ala-*Lys*-Thr-*Arg*-Ser-Ser-*Arg* (residues 9 to 20) and *Lys*-Ala-*Lys*-Gly-*Lys* (residues 125 to 129).

These basic clusters could be represented by the general formula $(X\text{-}A_q)_n$ where X = basic residue, A = non-basic residue, q = 1,2 and $n \geq 2$ (a multiplet structure corresponds to q = 0). Under these conditions a clustering percentage of about 85 p. cent can be calculated for histone F2a2.

A tentative delineation between interacting basic residues (located in basic clusters, q = 0 1,2) and non-interacting basic residues (singlets) has been performed for the main histone fractions (see table IV). 72 p. cent of the basic residues belong to the former type. The calculations allow one to predict that about 50 p. cent of the DNA phosphate groups are probably neutralized by direct electrostatic interaction with histone basic residues.

Recently, precise features have been derived from experimental evidence in relation to charge neutralization in chromatin histone-DNA complexes. It appears that both DNA and histones possess a substantial proportion of their potential binding groups in a free or unbound state [50].

TABLE IV.

Histone positive charge distribution in calf thymus chromatin.

Histone	F1	F2a1	F2a2	F2b	F3
Mol. weight.....(a)	[42] *ca* 21,000	[42] 13,300	[43] 14,005	[42] 13,770	[42] 15,229
M.....(b)	[44] 212–216	[47] 102	[43] 129	[46] 125	[45] 135
Positives charges/protein.....(c)	(d) 65–66	25	26	29	32
Positive charges in basic multiplets (q = 0).....(f)	(e) *ca* 31	15	6	15	16
Positive charges in basic clusters (q = 1,2).....(f)		5	15	3	11
Total positive charges in clusters (q = 0,1,2).....(f)	at least 31	20	21	18	27
Protein/DNA (weight/weight).....[48.49]	0.20	0.20	0.20	0.20	0.20

(a) from sequence determination (except for F1) disregarding acetyl and methyl residues.

(b) M = total number of residues.

(c) Lys and Arg residues, including the NH_2-terminal group in the case of F3 and F2b.

(d) calculated from amino-acid composition (see ref. [55]).

(e) assuming a clustering percentage, p = 47 p. cent, average value for the main histone fractions (see Table III).

(f) a basic cluster is defined by the sequence $(X\text{-}A_q)_n$, X = basic, A = non-basic, q = 0,1,2, $n \geq 2$.

(*) A weight ratio equal to 1 between DNA and acid-soluble proteins was assumed [49].

Titration measurements [51], as well as chemical [52] and enzymatic [53] modifications of chromatin, all indicate that about 20-30 p. cent of the lysyl and arginyl residues are unbound. This value is to be compared to the histone basic residues 28 p. cent of which belong to singlet structures.

Furthermore, it appears that large numbers of DNA phosphate groups (values up to 50 p. cent have been found) are free to interact with external cationic molecules [50]. It remains to be established if this portion of the DNA is found « throughout the length of a DNA-chain (e.g. one phosphate backbone free) or localized in patches where both phosphate chains are unbound alternating with areas of total binding » [50]. Experimental evidence on this point is still unclear. It appears likely that basic doublet structures link both phosphate chains through electrostatic interaction involving two « vertical » phosphate groups. Because of distance requirements (the maximum distance between both positively charged centers in the Lys-Lys doublet does not exceed 16 Å) ; the interaction certainly takes place in the minor groove.

Figure 17 presents a model for histone F2a1 interaction with DNA. It is assumed that all the basic residues in clustered basic regions (for definition see (f) in table IV) are in direct contact with DNA phosphate groups, whereas basic singlet structures are supposed not to interact with DNA. Under these conditions, histone F2a1 has about 4 Lys and Arg non-interacting residues among 25, yielding 16 p. cent free basic residues. The model makes apparent three important non-basic regions AB, BC and CD, located between the clustered basic regions A, B, C and D. It has usually been assumed that histones in chromatin interact with DNA at the basic ends of the molecules, leaving a central helical non-bound region [50]. Less sophisticated models have also been considered in the case of histone F2a1, assuming the existence of two very different parts in the molecule : the first half (amino terminal) contains the essential basic residues whereas the other residues are concentrated in the second half (carboxyl terminal) [4, 54]. However, the model proposed by Richards and Pardon [4] leaves the possibility of re-attachment of histone F2a1 to DNA by means of the basic residues 77, 78, 79 as well as those at positions 91, 92 and 95 which belong to the C-terminal part of the molecule. In agreement with this proposal, unpublished results by Palau *et al.* established that a 18 residue C-terminal peptide obtained from histone F2a1 by BrCN splitting is able to stabilize double stranded DNA against thermal denaturation. The eventual presence of loops of non-basic residues appearing between highly basic regions in histone F2a1, has already been considered by Phillips [56], as well as by Richards and Pardon [4]. However, these models do not distinguish basic residues located in multiplet structures from those located in singlet structures. Two extreme possibilities can be considered in the frame of the model features presented in figure 17 : either a fully extended structure so that non-basic regions do not protude from the DNA, or a compact structure where the same regions are included in external loops. The latter arrangement would lead to a weight ratio of histone F2a1 to DNA of about 2, whereas the former would afford values much lower than 1, e.g. 0.5 as calculated by

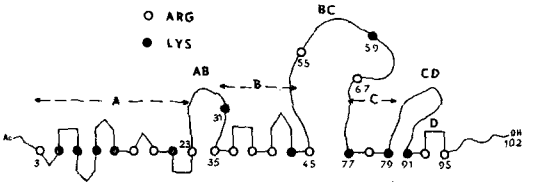

FIG. 17. — *Schematic representation of the structure of histone F2a1 interacting with double stranded DNA.* Horizontal circles represent basic residues, Arg (○) and Lys (●), on interaction with DNA phosphate groups. Two consecutive basic residues belonging to a multiplet structure (for definition see (f) in table IV) certainly interact with two « vertical » phosphate groups in the minor groove. No assumption is made about the secondary structure of protein intermediate regions such as AB, BC and CD.

Richards and Pardon [4]. Ratios (w/w) of about 1 observed in chromatin [49, 4] favours an intermediate situation, in which non-basic residues would interact with DNA (particularly the small loops in regions A, B and D ; see figure 17). This statement however is only valid if values for the individual histones making up the chromatin do not deviate significantly from the mean. This is not the case for histone F1, which certainly adopts a much more extended conformation. Secondary structure features of these non-basic regions have been considered. It has been emphasized that most of the BC region could be in an α-helical conformation [56, 4]. Smythies *et al.* [57] have even assumed the 33-98 part of histone F2a1 to be an α-helix. However, experimental results by Li et al. [58] indicated that only 17 residues of this histone were able to undergo a transition from a random-coil to an α-helix conformation, when the medium was saturated with phosphate anions, although it is possible that the amount of α-helix may be increased to a larger extent on interaction

with a specific DNA segment in chromatin. If histone F3 is analyzed on the same basis as histone F2a1, striking analogies do appear between both arginine-rich histones in the AB and CD regions. Primary structure analogies between calf-thymus F2a1 and F3 histones have been noticed previously by De Lange *et al.* [45] which suggest higher order structure analogies. In particular, the C, CD and D regions in both proteins (residues 75 to 95 and 113 to 131 of histones F2a1 and F3 respectively) as well as the A, AB and B regions (residues 16 to 45 and 14 to 37 of histones F2a1 and F3 respectively) show a great deal of sequence analogy.

In one sense, the interaction between histones (at least arginine-rich histones) could be visualized as involving two distinct types of region, a very basic one forming a continuous positive polyelectrolyte backbone in direct interaction with DNA phosphate groups, as in the case of protamines, and a less polar one which would be able to afford compact structures, such as in globular proteins. The histone external loops of defined tertiary structure within the chromosomal complex could act as sites of recognition between enzymes (acetylases, methylases...) and the nucleoprotein complex, as well as loci for intermolecular association (histone-histone interactions). Recent results by Krieger *et al.* [59] using F2a1 histone frag-

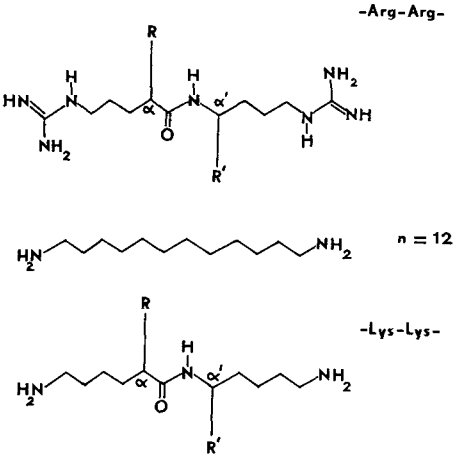

FIG. 18. — *Comparison between two peptide basic doublets* (-Arg-Arg- and -Lys-Lys-) and 1,12- diaminododecane.

ments have shown that calf-thymus deacetylase failed to remove acetyl groups when using a heptapeptide containing the Lys 16 residue, whereas large N-terminal fragments were active as substrates for the enzyme. It appears that a rather long sequence of the histone F2a1, including the AB region would be required for recognition by the deacetylating enzyme. Experiments using nitroxide spin labelling of calf thymus histone F3 showed that cysteinyl residues at positions 96 and 110 belong to a non-polar region of the protein which certainly adopts a precise tertiary structure [60]. This region appears analoguous to the BC region depicted in figure 17 for calf thymus histone F2a1. It is very interesting to note that the F2a1-like histone from male gonads of the

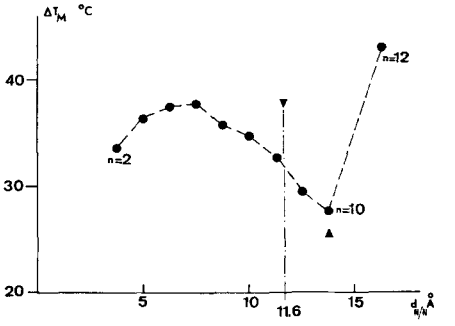

FIG. 19. — *Plot of* ΔT_M *versus the maximal distance* $d_{N/N}$ *between both the positively charged nitrogen centers in the following ligands :* (●) diamines of the series H_2N-$(CH_2)_n$-NH_2, n = 2-10 and 12, (▲) decamethonium and (▼) malouetine ($d_{N/N}$ = 11.6 Å).

sea-urchin *Parechinus angulosus* possesses a cysteinyl residue at position 73 [61] which appears to be analogous to cysteine 110 in calf thymus histone F3. This observation suggests that F2a1 and F3 histones have a common origin, and that the BC loop in histone F2a1 appears to be an appropriate region for tertiary structure.

Comparative thermal denaturation studies of DNA complexes with diamines of the series H_2N-$(CH_2)_n$-NH_2 and dibasic peptides clearly establish an analogy between both types of ligands (see fig. 1 and 2). The similitude in thermal behaviour, certainly reflects structural analogies. As shown in figure 18, the peptide basic doublets appear to be similar to the aliphatic diamine n = 12, as far as the distance $d_{N/N}$ between both the positively charged centers is concerned. Mahler and Mehrotra [30] and Tabor [62] have shown that the stabilization of the complexes defined by ΔT_M was dependent on $d_{N/N}$ for the series of aliphatic diamines, n = 2 - 10. When ΔT_M versus n was plotted a maximum was observed for n = 5 [30, 62]. The present work reports similar results obtained with the same series of diamines in a medium of different ionic strength. A maximum stabilization also appears when n = 5 (see figure 19). The analysis has been extended to 1-12-diaminododo-

cane, decamethonium and malouetine. A quantitative analysis was performed as described in table I. Figure 19 represents the variations of ΔT_M versus $d_{N/N}$, assuming the most extended all trans conformation for each diamine. It is likely that conformations with shorter distances are present when interaction with DNA takes place, especially for the larger n values. Malouetine, which is a rigid steroidal dicationic molecule (see formula in figure 9), has a well defined N/N distance, d *ca* 11.6 Å [29]. This molecule was chosen to standardize the curve in figure 19. It appears that ΔT_M is much greater for this rigid steroidal ligand than for non-rigid diamines of similar distance (n = 8 or 9). The difference is certainly not due to the presence of a quaternary ammonium cation ($C\text{-}\overset{+}{N}(CH_3)_3$) in the first case and an ammonium cation ($C\text{-}\overset{+}{N}H_3$) in the second one : decamethonium and 1, 10-diaminodecane do not differ significantly in their stabilizing effects (ΔT_M = 25.6° and 27.6° respectively, see table I). Under the same ionic strength conditions, 1,12-diaminododecane, affords a greater stabilization of the DNA complex, ΔT_M = 42.5°. The shape of the curve in figure 19 suggests that two stabilization maxima are present when DNA interacts with aliphatic diamines of the series $H_2N\text{-}(CH_2)_n\text{-}NH_2$. The first maximum at n = 5 ($d_{N/N}$ *ca* 7.5 A) may correspond to a charge neutralization between the ligand and two consecutive phosphates belonging to the same DNA strand, the second one appears at higher N/N distances (n *ca* 12) and might involve two « vertical » phosphates in different DNA strands. The distance between two consecutive phosphate atoms in the same strand is about 6.5 Å, whereas minimal distances between phosphates in two different strands are about 12 Å and 19 Å for the minor and major grooves respectively, when using coordinates for helical DNA as given by Langridge *et al.* [63] (*). This would imply that DNA retains its secondary structure during complexation. However, a DNA hyperchromic effect is observed in the UV spectrum at 258 nm when both ligands, n = 10 and n = 12, are added to DNA under isotherm conditions (*ca.* 22°C), suggesting conformational variations of the DNA bases. Other ligands with lower n values do not give rise to this hyperchromic mixing effect. In the case of steroidal diamine-DNA complexes, characteristic DNA changes in optical properties (UV and CD) were also reported by Mahler *et al.* [34]. Furthermore, the thermal behaviour of 1-12-diaminododecane and malouetine differs markedly from that found for shorter diamines (n = 2 - 10). A saturation curve ΔT_m versus ligand to DNA ratio is characteristic of the latter case (see fig. 1 as a representative example). Curves with a maximum (see figures 3 and 4) as observed in the former case, certainly correspond to the appearance of more than one complex when the ligand to DNA ratio is varied. ΔT_M (23.9°, see table I) for the peptide I-DNA complex appears to be quite different from that expected on the basis of structural analogies with diamine n = 12 (ΔT_M = 42.5°) as suggested in figure 18. It could be assumed that a conformational rearrangement is responsible for the lowering of ΔT_M. Peptide I appears to be more similar to diamine n = 10 (ΔT_M = 27.6°). Steric effects due to the substitution of both carbon atoms α and α' with bulky groups could favour conformations other than the all trans one depicted in figure 18. The thermal behaviour of peptide I-DNA complexes is of the normal type with a typical saturation curve ΔT_m versus ligand to DNA ratio. When other dibasic peptides, such as Lys-Lys and Arg-Lys were compared to peptide I, important differences in ΔT_M were again observed (34.6° and 30.6° respectively). In fact, different diamine configurations are possible for both compounds, (i) $N^{\alpha}/N^{\varepsilon}$ (first residue), (ii) $N^{\alpha}/N^{\varepsilon'}$ (second residue) and (iii) $N^{\varepsilon}/N^{\varepsilon'}$ Configuration (i) appears to be similar to that encountered in diamine n = 5 for which ΔT_M = 37.7°. On the basis of the above mentioned results the N/N distance appears to be an important parameter when dicationic ligands interact with helical DNA. However, this single parameter is not sufficient to explain the reported experimental results. In particular, the ΔT_M difference between a rigid dicationic ligand such as malouetine and a non-rigid one such as decamethonium cannot be only explained on the basis of a $d_{N/N}$ difference between both compounds. Both ligands differ strongly in the chemical nature of the molecule moiety located between the positively charged nitrogen centers. It is highly hydrophobic in the first case ($C_{21}H_{36}$, malouetine) and less hydrophobic in the second ($C_{10}H_{20}$, decamethonium). It might be also that the very pronounced hydrophobic character of 1,12-diaminododecane could contribute significantly to the thermal stabilization of DNA complexes, as the thermal behaviour of this diamine differs markedly from that of other aliphatic diamines in the series. Although peptide basic doublets may have conformations with N/N distances similar to that of diamine n = 12, they appear to be more polar because of the presence of the central amide bond.

(*) A recent refinement of the structure of B-DNA by Arnot and Hukins [64] retains essentially the same positions for the phosphate groups as in the model of Langridge *et al.*

II. — *DNA conformational changes induced by histones through localized interactions.*

The observation that coiling and uncoiling of circularly closed DNA's can be achieved by steroidal diamines appears to be very interesting [21, 31]. When bacteriophage PM2 DNA interacts with malouetine, reversible alterations of the superhelix structure similar to that found during the interaction with intercalating ligands are observed [31]. This effect is depicted in figure 8 were the malouetine-PM2 DNA system was analyzed using different ionic strength conditions from those used by Waring and Chisholm [31]. It was observed that 1-12-diaminododecane is also able to uncoil the superhelix structure of PM2 DNA as shown in figure 7. However, in comparison with the above steroidal ligand, no regeneration of the supercoil configuration is achieved even at very high ligand to DNA ratios. Nevertheless, the binding appears to be reversible as shown in experiments where the ionic strength is varied [65]. No uncoiling effect of PM2 DNA is observed when diamine n = 10 as well as decamethonium (see figures 5 and 6 respectively) are used as ligands.

Even if no detailed mechanism of the interaction between diamines and DNA is known up to now, it is likely that hydrophobic forces contribute to the total energy of interaction. It is interesting to note that in the case of the malouetine-DNA complex, characteristic proton groups (C-CH_3 at positions 18 and 19) belonging to the most hydrophobic part of the ligand molecule have a much shorter relaxation time T_2 than proton groups belonging to the polar part of it (see table II). This result can be tentatively interpreted as being the consequence of an approach of the steroidal ligand through its more bulky β-face. A close contact between hydrogens of the ligand C-CH_3 groups and CH_2 groups (probably at position 5') of DNA deoxyribose (and/or methyl groups of thymines) could explain the observed difference [66].

When interacting with DNA, malouetine and 1,12-diaminododecane certainly involve two distinct types of forces, electrostatic and hydrophobic.

In this light, partial histone sequences of the type $(X\text{-}A_q)_n$ where X = basic residue, A = non-polar residue, q = 1,2 and $n \geqslant 2$, could have a precise function. The non-polar residues A could interact with DNA through hydrophobic forces, in connection with electrostatic cohesion afforded by the adjacent basic residues.

A very particular basic region is that observed in histone F2a1 between residues 16 and 20 (—Lys—Arg—His—Arg—Lys—). There is an important clustering of basic residues and enzymatic modifications of the ε-amino groups by acetylation and methylation respectively occur in the lysine residues 16 and 20. The residues Arg and Lys, included in basic doublet structures, are certainly involved in a direct electrostatic interaction with DNA phosphate groups.

Interaction with histidine 18 may differ markedly, because of the lower pK value of this residue (imidazole group). Histidine could afford interactions with DNA, owing to the ability of the imidazole moiety to form hydrogen bonds (the bifunctionality of the group yields two possibilities for hydrogen bonding, as the $\diagup C = N—$ groupe could act as an electron donor and the $\diagdown N—H$ group as a proton donor).

When the complexes between histidinamide and sonicated DNA were analyzed by NMR, relaxation and chemical shift effects were observed (fig 13, 15 and 14). The system appears to be characterized by a high dissociation constant value even in a low ionic medium (see table II). When the DNA to ligand ratio is increased, both C_2-H and C_4-H imidazole protons are shifted to lower field, whereas β-CH_2 protons in the side-chain remain unaffected. NMR analysis of complexes between DNA and small molecules is characterized either by chemical shift effects (upfield or downfield) or by no shift effect. The latter case was observed for the malouetine-DNA system. Upfield effects have been reported and they have been related to the fact that the ligand is able to be intercalated between two consecutive base pairs [19, 67]. The downfield shift reported for the histidinamide-DNA system might be interpreted as due to the fact that the imidazole ring and a nucleic base lie in the same plane. Hydrogen bonding as depicted in figure 20 satisfies this geometrical condition. However, complex formation might also induce chemical shifts by variation of the imidazole pK even under constant pH conditions.

A model is presented to describe the interaction between DNA and the N-terminal part of histone F2a1 (residues 16 to 20). Evidence is derived from general chemical principles, model building as well as from the NMR results with histidinamide-DNA complexes reported above.

1) The positively charged side-chain guanidines and amino groups from residues Arg and Lys respectively, would lie in close contact with four

negatively charged phosphate groups belonging to different DNA strands. A similar arrangement was previously proposed by Richards and Pardon [4].

2) The peptide backbone between residues 16 and 20 of histone F2a1 is assumed to adopt a conformation such that the side-chaine of histidine 18 is directed towards the inner structure of DNA.

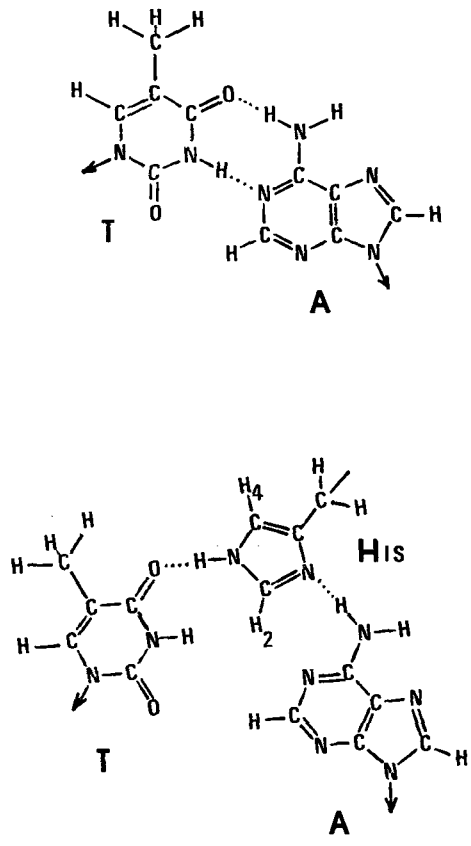

FIG. 20. — *Hydrogen bonding between the F2a1 histidine residue 18 and the components of a DNA base pair.* Upper part : Watson-Crick A.T base pair. Lower part : ternay complex between the imidazole moiety of the histidine residue, adenine and thymine.

3) Proximity between the $\rangle$NH and $\rangle$C = N— imidazole groups of histidine 18 and $\rangle$C = O and —NH_2 groups of the DNA bases could allow the formation of new hydrogen bonds yielding a ternary complex as shown in figure 20. Energy considerations suggest that an A.T pair should be more favoured than a G.C pair, as in the case of the former the two broken hydrogen bonds are fully re-established when interaction with His takes place. Experimental evidence for ternary complexes between histidine and nucleic acid bases is not available to our knowledge. It is, however, known that imidazole affords molecular crystals in which molecules interact in monodimensional chains through hydrogen bonding [68]. Owing to complex formation, the corresponding DNA base pair elements are probably displaced towards the periphery of the double helix. Under these conditions, bending or kinking of the DNA regular structure appears feasible as depicted in figure 21.

Inspection of molecular models (*) suggests that the imidazole group of His 18 in histone F2a1 can interact through hydrogen bonding with two nucleic base pairs as schematically depicted in figure 21.

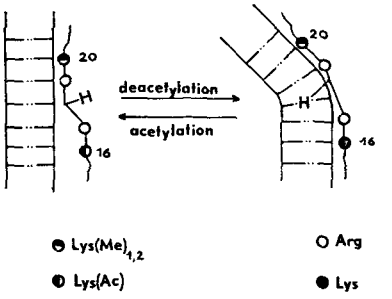

FIG. 21. — *Schematic DNA conformational changes induced by enzymatic acetylation and deacetylation of F2a1 lysine residue 16.*

The proposed mechanism affords a way of disrupting the double stranded DNA regular structure through a local nucleic acid-protein interaction. It provides no regular bending of the DNA, but rather a dislocation of the DNA secondary structure at specific points. This localized perturbation could be integrated in more or less complex tertiary structures.

According to the results of Richards and Pardon [4], histones involved in the maintainance of DNA tertiary structure in chromatin do contain His residues. In contrast, histone F1 which is not related to DNA folding, is devoid of this residue. It is not possible to assess if the mechanism is restricted to the single His residue 18 in histone F2a1. The presence of basic amino-acid residues adjacent to histidine appears to be essential as suggested by the respective affinities of a dicationic ligand (malouetine) and histidinamide

(*) One turn of double helical DNA and the N-terminal part of histone F2a1 (residues 1 to 22) were built using polysterene models according to the procedure of Thomas [69].

towards double stranded DNA. In the sequence —Lys—Arg—His—Arg—Lys—, the central His residue would be forced to interact with DNA, if only with low energy intermolecular forces, because of the presence of adjacent basic residues strongly interacting with DNA by means of electrostatic forces.

If the electrostatic interaction was altered, this could lead to the loss of the His-DNA interaction. Enzymatic modification of lysine ε-amino groups through acetylation is indeed observed for the arginine-rich histones F2a1 and F3, in relation to the control of genetic activity in the cells of higher organisms [70]. In calf thymus, acetylation and deacetylation of the residue lysine 16 appear to be the main enzymatic structural modifications of histone F2a1. By acetylation, the basic doublet —Lys—Arg— is transformed into a singlet —Lys (Ac)—Arg— yielding a reduced affinity between DNA and this region of the histone. As a consequence, the adjacent residue His 18 would lose its ability to interact with DNA bases by hydrogen bonding, so that a normal base pair could be re-established, followed by a DNA structural modifications.

DNA conformational changes induced by post-synthetic histone modifications, such as acetylation of the arginine-rich histones, could be related, among other things, to reversible chromatin changes from a condensed or « inactive » state to a diffuse or « active » one. It has been observed in some biological systems that acetylation indeed occurs at the boundaries between condensed and diffuse chromatin [70].

Acetylation and deacetylation of Lys 16 in histone F2a1 could correspond to a general switch mechanism involved in the control of genetic activity in the cells of higher organisms, by allowing reversible DNA conformational changes to occur. Specific interactions between chromosomal components could then take place, as a consequence of tertiary structure variations in large regions of DNA.

CONCLUSION.

An experimental strategy directed towards the understanding of the molecular organization of nucleoprotein complexes within chromatin has been developed.

Because of the heterogeneity in amino acid distribution along the sequence of histones, the study of independent protein portions seems relevant to features in the whole structure. Histone-like synthetic peptides, as well as chromosomal protein fragments appear therefore to be suitable models to analyze histone-DNA interactions in molecular terms.

Circularly closed DNA's also appear as adequate models for DNA in the chromosomes. Portions of chromosomal DNA could adopt topologically related structures [1].

ADDENDUM.

After this manuscript was written a paper by De Santis *et al.* (1974, *Biopolymers*, 13, 313-326) appeared on the interaction between DNA and the N-terminal portion of histone F2a1 (residues 16 to 20). Their conclusions were reached essentially on the basis of energy calculations. In some aspects they appear to be closely related to those presently reported : location of the peptide in the DNA minor groove, linking of both DNA strands by electrostatic interactions. However important differences do appear. The histidine residue 18 is supposed to interact by its imidazole moiety with a negatively charged phosphate group. No conformational changes are assumed for DNA when the interaction takes place.

A preliminary study by analytical ultracentrifugation of complexes between bacteriophage PM2 DNA and a histone-like synthetic peptide (Ac—Gly—His—Arg—Arg—ValNH_2) suggests that some sort of DNA packing occurs when molecules interact (unpublished result from our laboratory).

Acknowledgments.

We thank the staff of the Centre de Biochimie Macromoléculaire (C.N.R.S., Montpellier) for their skilful technical assistance, Dr B. R. Thomas (Chemical Center, The Lund Institute of Technology, Lund, Sweden) for laboratory facilities when building polysterene atomic models and Dr Barbara Dod for helping to correct our english.

RÉSUMÉ.

On décrit la dénaturation thermique de complexes formés entre ADN de thymus de veau et peptides basiques de synthèse (di-, tri- et tétra-peptides) possédant la structure X-X (doublet basique, X = Arg ou Lys) caractéristique des histones de structure primaire connue. Des analogies de comportement vis-à-vis de la dénaturation thermique entre ce type de peptides et des amines aliphatiques de la série $H_2N—(CH_2)_n—NH_2$ suggèrent qu'une structure à double charge avec une distance appropriée entre les deux centres portant les charges positives, est très adaptée pour interagir avec l'ADN dans sa conformation en double hélice.

Un modèle d'interaction entre histones et ADN est proposé sur la base des exigences stériques mentionnées (modèle diaminique) ; il est décrit en détail dans le cas de l'histone F2a1.

18 000 AUSSEDAT REY

Imprimé en France

Le rôle de processus enzymatiques d'acétylation et de désacétylation de certains résidus lysine dans le cas d'histones riches en arginine est discuté dans le cadre du modèle diaminique. Un rôle possible du résidu His 18 de l'histone F2a1 est envisagé en relation avec ce modèle.

Une étude par résonance magnétique protonique de complexes entre ADN et deux dérivés modèles, la malouétine (stéroïde ayant deux fonctions ammonium quaternaire) et l'histidinamide, montre qu'une description précise de ces complexes est possible du point de vue magnétique, thermodynamique et cinétique.

Des résultats préliminaires, ayant trait à l'étude par ultracentrifugation analytique de complexes entre l'ADN de bactériophage PM2, de structure circulaire fermée par covalence, et des diamines sont également discutés.

REFERENCES.

1. Crick, F. H. C. (1971) *Nature*, **234**, 25-26.
2. Ris, H. (1974) Chromosome Structure Symposium, Strasbourg, 6-7th April.
3. Du Praw, E. J. (1970) DNA and Chromosomes, Holt, Rinehart and Winston, Inc. New York.
4. Richards, B. M. & Pardon, J. F. (1970) *Expt. Cell. Res.*, **62**, 184-196.
5. Bram, S. & Ris, H. (1971) *J. Mol. Biol.*, **55**, 325-336.
6. Subirana, J. A. & Puigjaner, L. C. (1974) *Proc. Nat. Acad. Sci. USA*, **71**, 1672-1676.
7. Puigjaner, L. C. & Subirana, J. A. (1974) *J. Appl. Cryst.*, **7**, in the press.
8. Stellwagen, R. H. & Cole, R. D. (1969) *Annual Rev. Biochemistry*, **38**, 951-990.
9. Hnilica, L. S. (1972) The structure and biological Function of Histone, CRC Press, Cleveland Ohio, Chapter 6.
10. Shapiro, J. R., Leng, M. & Felsenfeld, G. (1969) *Biochemistry*, **8**, 3219-3232.
11. Brown, P. E. (1970) *Biochim. Biophys. Acta*, **213**, 282-287.
12. Cernosek, S. F. Jr., Malin, M., Wells, M. & Fasman, G. D. (1974) *Biochemistry*, **13**, 1252-1264.
13. Bartley, J. A. & Chalkley, R. (1972) *J. Biol. Chem.*, **247**, 3647-3655.
14. Boublik, M., Bradbury, E. M., Crane-Robinson, C. & Rattle, H. W. E. (1971) *Nature New Biology*, **229**, 149-150.
15. Bradbury, E. M. & Rattle, H. W. E. (1972) *Eur. J. Biochem.*, **27**, 270-281.
16. Fritzshe, H. (1972) *FEBS Letters*, **23**, 105-106.
17. Gabbay, E. J., Sanford, K. & Baxter, C. S. (1972) *Biochemistry*, **11**, 3429-3455.
18. Gabbay, E. J., Sanford, K., Baxter, C. S. & Kapicak, L. (1973) *Biochemistry*, **12**, 4021-4029.
19. Dimicoli, J. L. & Helene, C. (1974) *Biochemistry*, **13**, 714-723 and 724-730.
20. Bauer, W. & Vinograd, J. (1971) in *Progress in Molecular and Subcellular Biology*, ed. Hahn, F. E., Springer Verlag, 181-215.
21. Waring, M. (1971) in *Progress in Molecular and Subcellular Biology*, ed. Hahn, F. E., Springer Verlag, 216-231.
22. Barclay, A. B. & Eason, R. (1972) *Biochim. Biophys. Acta*, **269**, 37-46.
23. Marmur, J. (1961) *J. Mol. Biol.*, **3**, 208-218.
24. Merrifield, R. B. (1969) *Advan. Enzymol.*, **32**, 221-296.
25. Winkler, H. U. & Beckey, H. D. (1972) *Biochem. Biophys. Res. Comm.*, **46**, 391-398.
26. Waring, M. J. (1970) *J. Mol. Biol.*, **54**, 247-279.
27. Crothers, D. M., Kallenbach, N. R. & Zimm, B. H. (1965) *J. Mol. Biol.*, **11**, 802-820.
28. Lazurkin, Y. S., Frank-Kamenetskii, M. D. & Trifonov, E. N. (1970) *Biopolymers*, **9**, 1253-1306.
29. Mahler, H. R., Goutarel, R., Khuong-Huu, Q. & Truong Ho, M. (1966) *Biochemistry*, **5**, 2177-2191.
30. Mahler, H. R. & Mehrotra, B. D. (1963) *Biochim. Biophys. Acta*, **68**, 211-233.
31. Waring, M. J. & Chisholm, J. W. (1972) *Biochim. Biophys. Acta*, **262**, 18-23.
32. Crothers, D. M. (1968) *Biopolymers*, **6**, 575-584.
33. Parello, J., Cavé, A., Puigdomenech, P., Maury, C., Capony, J. P. & Pechere, J. F. (1974) *Biochimie*, **56**, 61-76.
34. Mahler, H. R., Green, G., Goutarel, R. & Khuong-Huu, Q. (1968) *Biochemistry*, **7**, 1568-1582.
35. Gabbay, E. J. & Glaser, R. (1971) *Biochemistry*, **10**, 1665-
36. Spotswood, T. M., Evans, J. M. & Richards, J. H. (1967) *J. Am. Chem. Soc.*, **89**, 5052-5054.
37. Roberts, G. C. K. & Jardetzky, O. (1970) *Adv. Prot. Chem.*, **24**, 447-545.
38. Binsch, G. (1968) in *Topics in stereochemistry*, Ed. Allinger, E., John Wiley, New York, **3**, 97-192.
39. Ref. 9, pp. 16-28.
40. Parello, J. & Chevalet, C., unpublished.
41. Ref. 9, p. 19.
42. Ref. 9, pp. 47-49.
43. Sautière, P., Tyrou, D., Laine, B., Nizon, J., Puffin, P. & Biserte, G. (1974) *Eur. J. Biochem.*, **41**, 563-576.
44. Bustin, M. & Cole, R. D. (1969) *J. Biol. Chem.*, **244**, 5291-5294.
45. De Lange, R. J., Hooper, J. A. & Smith, E. L. (1973) *J. Biol. Chem.*, **218**, 3261-3274.
46. Iwai, K., Ishikawa, K. & Hayashi, H. (1970) *Nature*, **226**, 1056-1058.
47. De Lange, R. J., Fambrough, D. M., Smith, E. L. & Bonner, J. (1968) *J. Biol. Chem.*, **243**, 5906-5913.
48. Elgin, S. C. R., Froehner, S. C., Smart, J. E. & Bonner, J. (1971) *Advan. Cell. Mol. Biol.*, **1**, 1-57.
49. Itzhaki, R. F. & Cooper, H. K. (1973) *J. Mol. Biol.*, **75**, 119-128.
50. Simpson, R. T. (1973) *Advances in Enzymology*, **38**, 41-108.
51. Walker, I. O. (1965) *J. Mol. Biol.*, **14**, 381-398.
52. Simpson, R. T. (1971) *Biochemistry*, **10**, 4466-4470.
53. Simpson, R. T. (1972) *Biochemistry*, **11**, 2003-2008.
54. Ziccardi, R. & Schumaker, V. (1973) *Biochemistry*, **12**, 3231-3225.
55. Ref. 9, p. 7.
56. Phillipps, D. M. P. (1971) *Histones and Nucleohistones*, Ed. by Phillips, D. M. P. Plenum Press, London and New York, 47-83.
57. Smythies, J. R., Bennington, F. & Morin, R. D. (1972) *J. Theor. Biol.*, **37**, 151-158.
58. Li, H. J., Wickett, R., Craig, A. M. & Isenberg, I. (1972) *Biopolymers*, **11**, 375-397.
59. Krieger, D. E., Levine, R., Merrifield, R. B., Vidali, G. & Allfrey, V. G. (1974) *J. Biol. Chem.*, **249**, 332-334.
60. Palau, J. & Padros, E. (1972) *FEBS Letters*, **27**, 157-160.
61. Strickland, W. N., Strickland, M., Brandt, W. F., Morgan, M. & Van Holt, C. (1974) *FEBS Letters*, **40**, 161-166.
62. Tabor, H. (1962) *Biochemistry*, **1**, 496-501.
63. Langridge, R., Marvin, D. A., Seeds, W. E., Wilson, H. R., Hooper, C. W. & Wilkins, M. H. F. (1960) *J. Mol. Biol.*, **2**, 38-64.
64. Arnott, S. & Hukins, D. W. L. (1973) *J. Mol. Biol.*, **81**, 93-105.
65. Etienne, G., Raynaud, A. & Parello, J. (in preparation).
66. Puigdomenech, P., Cavé, A. & Parello, J. (in preparation).
67. Heller, M. J., Tu, A. T. & Maciel, G. E. (1974) *Biochemistry*, **13**, 1623-1631.
68. Gloux, P. & Lamotte, B. (1972) *Mol. Phys.*, **24**, 23-32.
69. Thomas, B. R. (1970) *Biochem. Biophys. Res. Comm.*, **40**, 1289-1296.
70. Allfrey, V. G. (1971) *Histones and Nucleohistones*, Ed. by Phillips, D. M. P., Plenum Press, London and New York, 241-294.